Anomalously large intermixing in aluminum–transition-metal bilayers

J. D. R. Buchanan, T. P. A. Hase, and B. K. Tanner
Department of Physics, University of Durham, South Road, Durham, DH1 3LE, United Kingdom

P. J. Chen, L. Gan, C. J. Powell, and W. F. Egelhoff, Jr.
National Institute of Standards & Technology, Gaithersburg, Maryland 20899

(Received 31 May 2002; revised manuscript received 5 August 2002; published 27 September 2002)

Intermixing has been studied in thin films of the form X/Al and Al/X, where X represents the transition metals in rows 4, 5, and 6 of the periodic table. Samples were grown by dc magnetron sputter deposition at room temperature and investigated using grazing-incidence x-ray reflectometry. Scans of the specular reflectivity have been fitted to determine the total interface width. We deduce the intermixing profile at the interface and separate it from the topographical roughness. Here intermixing has been measured in the great majority of the systems, and we find that there is a wide range in the extent of the intermixing. We bring to the attention of the thin-film community the surprisingly large degree of intermixing at room temperature in many cases. This phenomenon is not predicted by bulk diffusion parameters.

DOI: 10.1103/PhysRevB.66.104427 PACS number(s): 75.70.−i

Deposition of thin films of aluminum is key to a variety of technologies. Such films are used, for example, as conductors and passivators and in the fabrication of advanced sensors such as magnetic tunnel junctions (MTJ's). To date, much attention has been paid to the study of tunnel barrier properties and their evolution throughout the fabrication process. The barriers are known to contain defects, some natural[1] and others of artificial[2,3] origin. Factors such as barrier roughness[4] and chemical homogeneity[5] have been investigated as well as the specifics of barrier oxidation.[6]

There is currently much interest in producing MTJ's with thinner Al_2O_3 tunnel barriers to achieve lower device resistivities and higher values of the magnetoresistance.[7,8] However, for barriers less than ~8 Å thick, pinholes in the Al_2O_3 reduce the magnetoresistance sharply. As a result, there is much interest in identifying any nonideal aspects to barrier growth.

The barrier is grown by depositing an Al film on a ferromagnetic film and then oxidizing the Al film either with O_2 or with an oxygen plasma. One tricky aspect of barrier growth is to oxidize all the Al and none of the ferromagnet. This goal may be difficult to achieve if there is any mixing at the interface. Consequently, it is of much interest to investigate any intermixing that may occur when the Al film is deposited on the ferromagnet. Such was the initial motivation of the present work. However, the surprisingly large extent of the intermixing, in some cases, led us to expand the study to nonmagnetic metals. Al and transition-metal films are widely used in device technologies, and knowledge of the interface widths in these systems should promote a deeper understanding of the growth and subsequent device optimization. This paper presents a systematic study of the intermixing length in sputter-deposited Al–transition-metal films, most of which were previously unexplored. It is the first step in an ongoing study towards understanding fully such systems.

The samples were made at the National Institute of Standards and Technology (NIST) by dc magnetron sputtering using 2 mTorr (0.27 Pa) Ar. Metal bilayers were deposited at room temperature on substrates consisting of a silicon wafer with a ~3000-Å thermal oxide at the surface. All depositions were at normal incidence and with a magnetron power of 200 W at 350 V. The target to substrate distance in the sputtering system is unusually long, 18 cm, compared to a more typical value of 4 cm. For each transition metal two samples were prepared: X deposited on Al and Al deposited on X. The nominal structure for the majority of these samples consisted of 50 Å of each layer; however, for highly reactive samples thicknesses of 100 Å and even 200 Å of each layer were used.

Grazing-incidence x-ray reflectivity (GIXR) measurements were made at Station 2.3 of the Daresbury Synchroton Radiation Source and on a Bede GXR1 reflectometer in the Durham laboratory. The specular profile provides averaged in-plane structural information as a function of depth, such as layer thickness and total interface width σ_T. Analysis of the diffuse scatter, which arises from the topological roughness at the interface, allowed us to resolve the total interface width into separate components of topological roughness σ and intermixing parameter Σ, with each assumed to have an error function distribution. The components add in quadrature ($\sigma_T^2=\Sigma^2+\sigma^2$). Using the layer thickness parameters and total interface width σ_T derived from the best-fit model to the specular scatter, we can deduce the topological roughness σ by fitting to the diffuse scatter. Hence, the intermixing parameter Σ can be extracted. Note that when Σ exceeds σ by greater than a factor of about 3, the contribution of the topological roughness σ to the total interface width σ_T is small (less than 5.5%).

The specular data have been fitted using the *Bede REFS* MERCURY *code*.[9] The program uses a genetic algorithm to achieve a best fit between the data and that simulated for a model structure within the distorted-wave Born approximation. Within this code, the interface profile follows an error function and it was sometimes necessary to introduce extra compound layers to provide an accurate fit. The diffuse scatter was modeled by the Bede REFS code,[10] which uses a fractal model[11] to describe the individual interfaces.

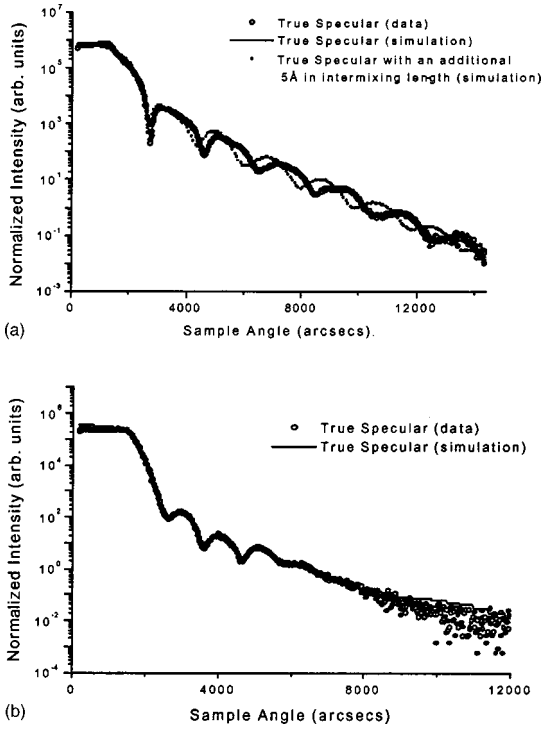

FIG. 1. Specular profile and simulated fit for films with nominal structures (a) SiO_2/Pt(50 Å)/Al(50 Å) and (b) SiO_2/Al(50 Å)/Pt(50 Å). Measurements made at a wavelength of 1.3 Å.

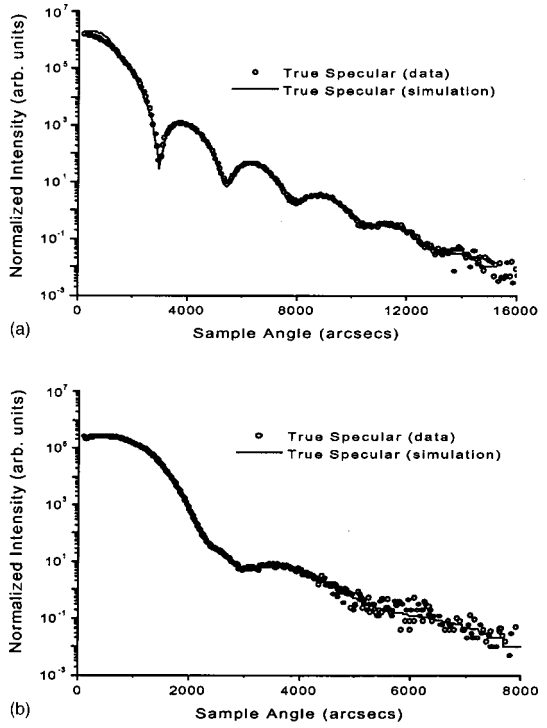

FIG. 2. Specular profile and simulated fit for films with nominal structures (a) SiO_2/Mo(50 Å)/Al(50 Å) and (b) SiO_2/Al(50 Å)/Mo(50 Å). Measurements made at a wavelength of 1.3 Å

TABLE I. Modeling parameters for films with nominal structures: (a) SiO_2/Pt(50 Å)/Al(50 Å) and (b) SiO_2/Al(50 Å)/Pt(50 Å). The "interface width" refers to the interface at the top of the indicated layer and includes both intermixing and topological roughness.

Layer	Thickness (Å)	Interface width (Å)
	(a) SiO_2/Pt/Al	
SiO_2		4
Pt	54	12
Al(0.5)Pt(0.5)	11	4
Al	39	5
AlO_2	17	7
	(b) SiO_2/Al/Pt	
SiO_2		3
Al	24	3
Al(0.2)Pt(0.8)	37	16
Pt	61	11
PtO_2	22	11

Modeling of the diffuse scatter using REFS is time-consuming and we find that $\sigma \ll \Sigma$ in all cases. In most instances we have therefore used the diffuse (I_{diff}) and specular (I_{spec}) intensities, integrated with respect to the in-plane component of the scattering vector q_x, within the Born wave approximation to deduce an average interface roughness $\langle\sigma\rangle$, which is then used to correct the specular data. Explicitly

$$I_{\mathrm{Diff}}/I_{\mathrm{spec}} = \exp(q_z^2\langle\sigma\rangle^2) - 1, \tag{1}$$

where q_z is the out-of-plane component of the scattering vector.

As examples from the large data set collected, specular profiles with their corresponding fits for the Pt and Mo sample sets are presented in Figs. 1 and 2. The specular data have been corrected for the effect of forward diffuse scatter by subtraction of the intensity in a similar θ–2θ scan made with the specimen offset by $-0.1°$ from the specular condition. Well-defined features observed in the Al grown on Pt sample [Fig. 1(a)] indicate immediately a greater degree of structural definition and thus a lower degree of mixing across the interface in comparison to the sample grown with Pt on

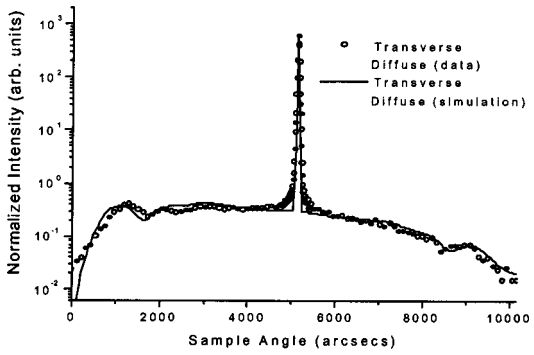

FIG. 3. Transverse diffuse scan and simulated fit at fixed q_z across the peak of a Kiessig fringe for SiO_2/Pt(50 Å)/Al(50 Å).

TABLE II. Resolved components of topological roughness σ and intermixing Σ, used to model the transverse diffuse fit seen in Fig. 3.

Layer	Topological roughness σ (Å)	Intermixing parameter Σ (Å)
SiO_2	1.1	3.4
Pt	3.4	11.5
Al(0.5)Pt(0.5)	1.1	3.8
Al	1.4	4.8
AlO_2	2.5	6.5

Al [Fig. 1(b)]. The models used for the specular fits seen in Fig. 1 are presented in Table I. To illustrate the sensitivity of the technique, an Al on Pt sample has been simulated with an additional 5 Å of $Al_{50}Pt_{50}$ at the interface. The specular profiles for Al on Mo and Mo on Al have similar characteristics. These two examples are in no way outstanding within the data set.

Scans of the specimen with respect to fixed detector were taken across both a maximum and minimum in the Kiessig interference fringes, transversely in reciprocal space. An example of such a transverse (rocking curve) scan of Al on Pt is given in Fig. 3. The solid line is a fit to the data using the parameters listed in Table II, and we note that the sum in quadrature of the topological roughness σ and intermixing parameter Σ is consistent with the total interface width deduced from the specular scatter [Table I(a)]. At all interfaces $\sigma \ll \Sigma$. The in-plane correlation length of 200 Å is of the order of the grain size observed in most sputtered materials and the fractal parameter of 0.8 represents a nearly two-dimensional fractal interface.

Data have been taken for all metals in groups 3, 4, and 5 of the periodic table (which the exception of Tc, which is radioactive). The intermixing lengths deduced from the analysis are presented in Table III. We have defined the total intermixing length as the sum of the mixing across all modeled interfaces between Al and *X*, plus the thickness of any extra compound layers

The intermixing lengths in these sputtered polycrystalline Al films listed in Table III are considerably larger than those obtained by Smith and co-workers.[12–14] where an ion-beam scattering technique was used to investigate low-index single crystals of Al. Further, the variation in intermixing length from one system to another is very large. There is also a striking difference in mixing length between samples of Al on *X*, and *X* on Al. In all cases, the intermixing lengths for Al on *X* are considerably smaller than those for *X* on Al.

The accuracy of the measurements listed in Table III depends on the extent of the intermixing and is set by the precision in fitting the specular profile to a chosen model. Samples with relatively little mixing have a well-defined layered structure, which is noted through the strong features observed in the specular profile [see Figs. 1(a) and 2(a)]. The fitting software provides a higher degree of accuracy with such profiles and precise values for the interface width are seen. As an example, the intermixing length for Al on Co has been found to be 8 ± 1 Å with five independent samples grown in more than one laboratory. Samples with a relatively large amount of intermixing have a greater uncertainty. A study of several Ru on Al samples gave an intermixing length of 52 ± 10 Å. The highly reactive Ag on Al system gave values of 45 and 64 Å for nominally identical samples.

We are unable to present a model to explain fully the experimental results. The only correlation found between intermixing length and bulk parameters was between cohesive energy and the intermixing length, as illustrated in Fig. 4. The plot shows a general decrease in intermixing length with increasing cohesive energy for sample types Al on *X* (*X* on Al reveals a very similar trend). Heats of alloying taken from de Boer[15] based on Miedema's model for 1:1 alloys, show no correlation with intermixing length.

TABLE III. The intermixing length, in Å, for transition metals (from groups 3, 4, and 5) grown on Al and Al grown on transition metals.

Ti		V		Cr		Mn		Fe		Co		Ni		Cu	
Al on Ti	Ti on Al	Al on V	V on Al	Al on Cr	Cr on Al	Al on Mn	Mn on Al	Al on Fe	Fe on Al	Al on Co	Co on Al	Al on Ni	Ni on Al	Al on Cu	Cu on Al
17	50	26	94	5	33	104	151	9	21	8	68	14	79	28	168
Zr		Nb		Mo		Tc		Ru		Rh		Pd		Ag	
Al on Zr	Zr on Al	Al on Nb	Nb on Al	Al on Mo	Mo on Al			Al on Ru	Ru on Al	Al on Rh	Rh on Al	Al on Pd	Pd on Al	Al on Ag	Ag on Al
10	51	8	36	13	34			8	52	4	47	48	56	25	45
Hf		Ta		W		Re		Os		Ir		Pt		Au	
Al on Hf	Hf on Al	Al on Ta	Ta on Al	Al on W	W on Al	Al on Re	Re on Al	Al on Os	Os on Al	Al on Ir	Ir on Al	Al on Pt	Pt on Al	Al on Au	Au on Al
20	44	1	9	1	35	21	86	1	71	2	54	19	45	52	63

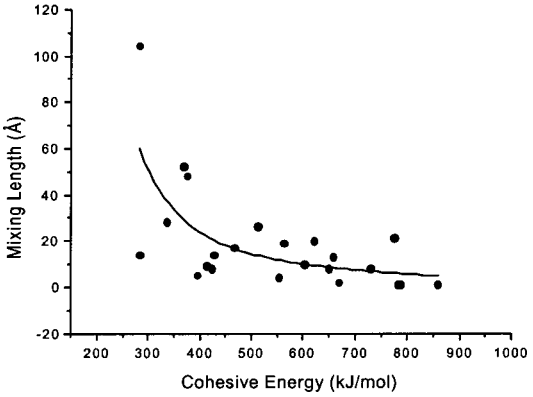

FIG. 4. The correlation between the intermixing length and the cohesive energy of element *X* in the sample set Al on *X* with an exponential fit as a ''guide to the eye.''

It is unlikely that energetic atoms produced in the sputtering process contribute appreciably to intermixing. In the deposition system, the large distance between the target and substrate (18 cm) is equivalent to approximately 10 mean free paths in the sputtering gas at 2 mTorr. The resulting ~100 collisions with Ar atoms and ions will thermalize essentially all sputtered atoms before they reach the substrate. The largest atomic diameter is 1.67 Å for Hf, the smallest is 1.24 Å for Ni, and thus to first order, the mean free path is independent of element. Even the row-6 atoms, which have the greatest mass, should be well thermalized in 100 collisions. We note that, on average, more mixing is observed in row 4 than in row 6, even though light atoms thermalize with fewer collisions. Thus, we see no evidence that high-energy impact accounts for the large amount of intermixing observed.

Furthermore, bulk interdiffusion rates of the thermalized atoms cannot account for the observed intermixing lengths. From published values of the activation energy and via the Arrhenius equation, the diffusion rate from one atomic species into another can be calculated. Using data in *Smithells Metals Reference Book*,[16] we find that the bulk diffusion parameters show no correlation with the observed intermixing length and do not predict such large intermixing at room temperature. The stability of the samples also supports the view that bulk diffusion rates do not determine the intermixing length. For example, an Al/Co sample showed no noticeable change in interface structure after one year. Grain boundary and surface diffusion processes, which are generally much more facile, seem to be responsible for intermixing during the deposition process.

Specular reflectivity measurements provide no information on the in-plane interface structure and so the measured intermixing length is therefore an average across the sample. Diffuse scatter is not sensitive to grain boundary density but influences such as local penetration along grain boundaries are unlikely to be sufficiently large to account for the wide variation in the intermixing length.

The asymmetry observed in the intermixing lengths between Al on *X* and *X* on Al is consistent with the interface asymmetry found recently by Bigault *et al.*[17] in Ni/Au multilayers and Luo *et al.*[18] in NiFe/Cu multilayers, both using anomalous x-ray scattering. Bigault *et al*. suggest that such an asymmetry indicates that dynamical (out-of-equilibrium) segregation driven by the growth front probably determines the intermixing length. Colgan and collaborators have studied the interdiffusion on annealing in thin films of Ni/Al,[19] Pt/Al,[20] and Pd/Al.[21] In all cases, interdiffusion proceeds via intermetallic compound formation but the minimum reaction temperature was found to be 300 °C for Ni/Al, 225 °C for Pt/Al, and 250 °C for Pd/Al.

The intermixing lengths and any associated asymmetry of the unannealed samples, grown below 60 °C, were not determined from the Rutherford backscattering data presented. Our data, using GIXR techniques to examine the surface average intermixing in almost the whole series of sputtered Al/transition-metal bilayers, represent hitherto unknown information that is highly relevant to the thin-film community. The surprisingly large degree and wide range of intermixing at room temperature, are not predicted by bulk diffusion parameters and we believe not generally appreciated.

The authors gratefully acknowledge the support of Chiu Tang, Station 2.3 at Daresbury SRS and the financial support from EPSRC and Seagate Technology. B.K.T. thanks the Leverhulme Trust for financial support.

[1] C. He Shang, J. Nowak, R. Jansen, and J. S. Moodera, Phys. Rev. B **58**, R2917 (1998).
[2] R. Jansen and J. S. Moodera, J. Appl. Phys. **83**, 6682 (1998).
[3] E. Yu. Tsymbal and D. G. Pettifor, J. Appl. Phys. **85**, 5801 (1999).
[4] V. Da Costa, F. Bardou, C. Béal, Y. Henry, J. P. Bucher, and K. Ounadjela, J. Appl. Phys. **83**, 6703 (1998).
[5] R. C. Sousa, J. J. Sun, V. Soares, P. P. Freitas, A. Kling, M. F. da Silva, and J. C. Soares, Appl. Phys. Lett. **73**, 3288 (1998).
[6] J. S. Moodera, E. F. Gallagher, K. Robinson, and J. Nowak, Appl. Phys. Lett. **70**, 3050 (1997).
[7] J. S. Moodera, L. R. Kinder, T. M. Wong, and R. Meservey, Phys. Rev. Lett. **74**, 3273 (1995).
[8] S. S. P. Parkin, K. P. Rocke, M. G. Samant, P. M. Rice, R. B. Beyers, R. E. Scheuerlein, E. J. O'Sullivan, S. L. Brown, J. Bucchigano, D. W. Abraham, L. Yu, M. Rooks, P. L. Trouilloud, R. A. Wanner, and W. J. Gallagher, J. Appl. Phys. **85**, 5828 (1999).
[9] M. Wormington, C. Pannacione, K. M. Matney, and D. K. Bowen, Philos. Trans. R. Soc. London, Ser. A **357**, 2827 (1999).
[10] M. Wormington, I. Pape, T. P. A. Hase, B. K. Tanner, and D. K. Bowen, Philos. Mag. Lett. **74**, 211 (1996).
[11] S. K. Sinha, E. B. Sirota, S. Garoff, and H. B. Stanley, Phys. Rev. B **38**, 2297 (1988).
[12] N. R. Shivaparan, M. A. Teter, and R. J. Smith, Surf. Sci. **476**, 152 (2001).
[13] V. Shutthanandan, A. A. Saleh, and R. J. Smith, Surf. Sci. **450**,

204 (2000).
[14] R. J. Smith, A. W. D. Vandergon, and J. F. Vanderveen, Phys. Rev. B **38**, 12 712 (1988).
[15] F. R. de Boer, *Cohesion in Metals* (North Holland, Amsterdam, 1998).
[16] E. A. Brandes and G. B. Brook, *Smithells Metals Reference Book*, 7th ed. (Butterworth-Heinemann, Oxford, 1992).
[17] T. Bigault, F. Bocquet, S. Labat, O. Thomas, and H. Renevier, Phys. Rev. B **64**, 125414 (2001).
[18] G. M. Luo, Z. H. Mai, T. P. A. Hase, B. D. Fulthorpe, B. K. Tanner, C. H. Marrows, and B. J. Hickey, Phys. Rev. B **64**, 245404 (2001).
[19] E. G. Colgan, M. Nastasi, and J. W. Mayer, J. Appl. Phys. **58**, 4125 (1985).
[20] E. G. Colgan, J. Appl. Phys. **62**, 1224 (1987).
[21] E. G. Colgan, J. Appl. Phys. **62**, 2269 (1987).